Supplementary materials

I. Pressure sensor calibration

Our analysis is based on identification of the onset and offset of the inhalation relatively to the electrophysiological recordings. Onset and offset of inhalation are the moments when the flow in the nose changes sign from outflow to inflow and vice versa. Airflow in the nose is proportional to the pressure difference due to the effective flow impedance of the nasal cavity. The Bernoulli effect is negligibly small. The moment of zero airflow velocity corresponds to zero pressure drop between the point of canula insertion and outside atmosphere. Thus inhalation and exhalation onsets occur at negative- and positive-going zero-crossings in the pressure signal, respectively. However, the pressure that is registered on the transducer is delayed relatively to the pressure in the nose due to two factors. First, thin and long capillary and a volume around the pressure sensor create a delay. Second, the hardware in line low pass filter (50 Hz), which has been used to reduce the electrical noise also adds some time delay. To account for such delays, we calibrated the pressure signal against instantaneous velocity measurement.

We compared the pressure signal from our sensor, exactly in the way it was used to measure sniffing, with a velocity signal measured by hot wire anemometer (HWA) (mini CTA 5439, Dantec Dynamics, Denmark). HWA measures the absolute velocity with very fast response time (less than 1 ms). We positioned the HWA adjacent to the point of canula insertion in a tube. We delivered controlled airflow to the tube by periodic movement of 6" loudspeaker, which was connected to the tube by plastic funnel and thin flexible tubing. The signal from HWA is an instantaneous rectified velocity signal, while the signal from pressure transducer reflects the time shifted bipolar velocity signal delayed relatively to instantaneous signal (Supplementary Fig. 1a). The zero crossing of the pressure signal is delayed by a constant time interval, Δt, relatively to the minima of HWA signal, which corresponds to zero velocity. For 4 Hz driving frequency the delay is approximately 32 ms.

This delay depends slightly on frequency (Supplementary Fig. 1a). However for the range of the sniffing frequencies we observed, 4.3±2.1 Hz (mean±std), the pressure signal delay changes very little: 32.2±1.9 ms. These changes (±2 ms) are significantly smaller than the duration of the sniffing cycle and inhalation phase. We also checked that the time delay does not depend on the amplitude of the periodic signal (data not shown). Thus, we assume the constant time shift equal 31ms between the pressure signal zero crossing and onset of inhalation. All the data was corrected by constant temporal shift of the sniffing signal relative to the e-phys recording data.

None of the conclusions of the paper depend on the exact position of the onset of the inhalation. Correcting for the temporal delay only shifts the response latency distribution toward later moments. The distribution is broad, tiling the sniff cycle. Precision and information content of the neuronal responses does not change if we move the change the position of the onset and offset of inhalation for ±2 ms.

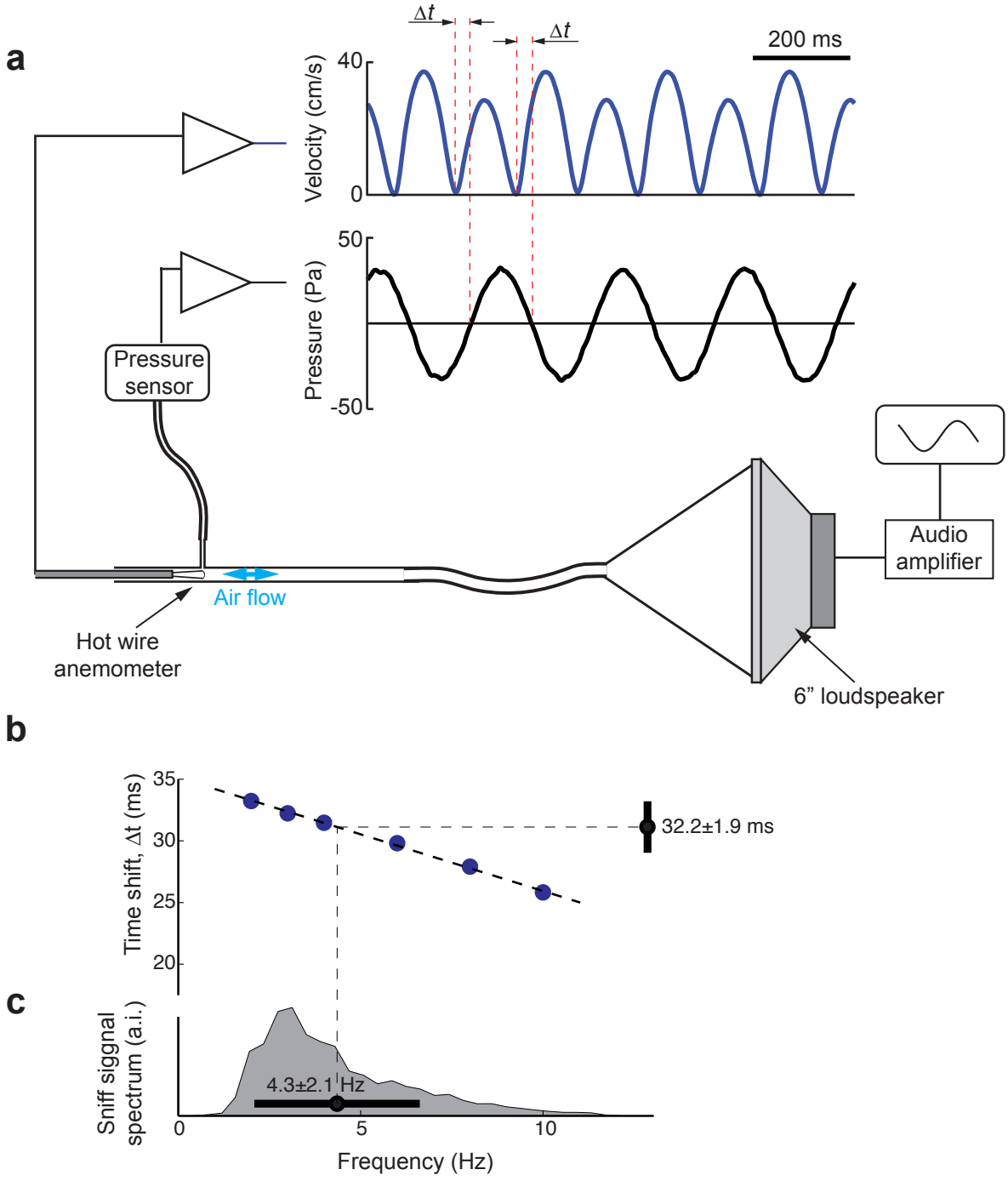

Supplementary Figure 1. Pressure sensor calibration. **a.** Schematics and example raw data for pressure sensor calibration. The pressure sensor was connected to a cannula, identical to that implanted to the mouse nose, by thin capillary. The cannula was inserted into a 2.4 mm ID tube. To simultaneously measure flow velocity in the tube, a hot wire anemometer was positioned inside the tube, near the insertion point of the cannula. The airflow inside the tube was driven by sine-wave movement of a 6" loudspeaker, which was connected to the tube by plastic funnel and short flexible tubing. The loudspeaker was controlled by function generator through an audio amplifier. The signal from pressure sensor and hot wire anemometer are shown above the schematics for a driving frequency 4 Hz. The pressure signal is delayed compared to velocity rectified signal for Δt=32 ms. **b.** The dependence of time shift between pressure signal and velocity signal as a function of frequency (blue dots). Dashed line is a linear fit. **c.** Distribution of sniffing frequencies for all mice used in the experiment. Average and standard deviation of the sniffing frequency are 4.3±2.1 Hz correspond to average time shift of 32.2±1.9 ms.

Nature Neuroscience doi:10.1038/nn.2877

II. Sniff analysis

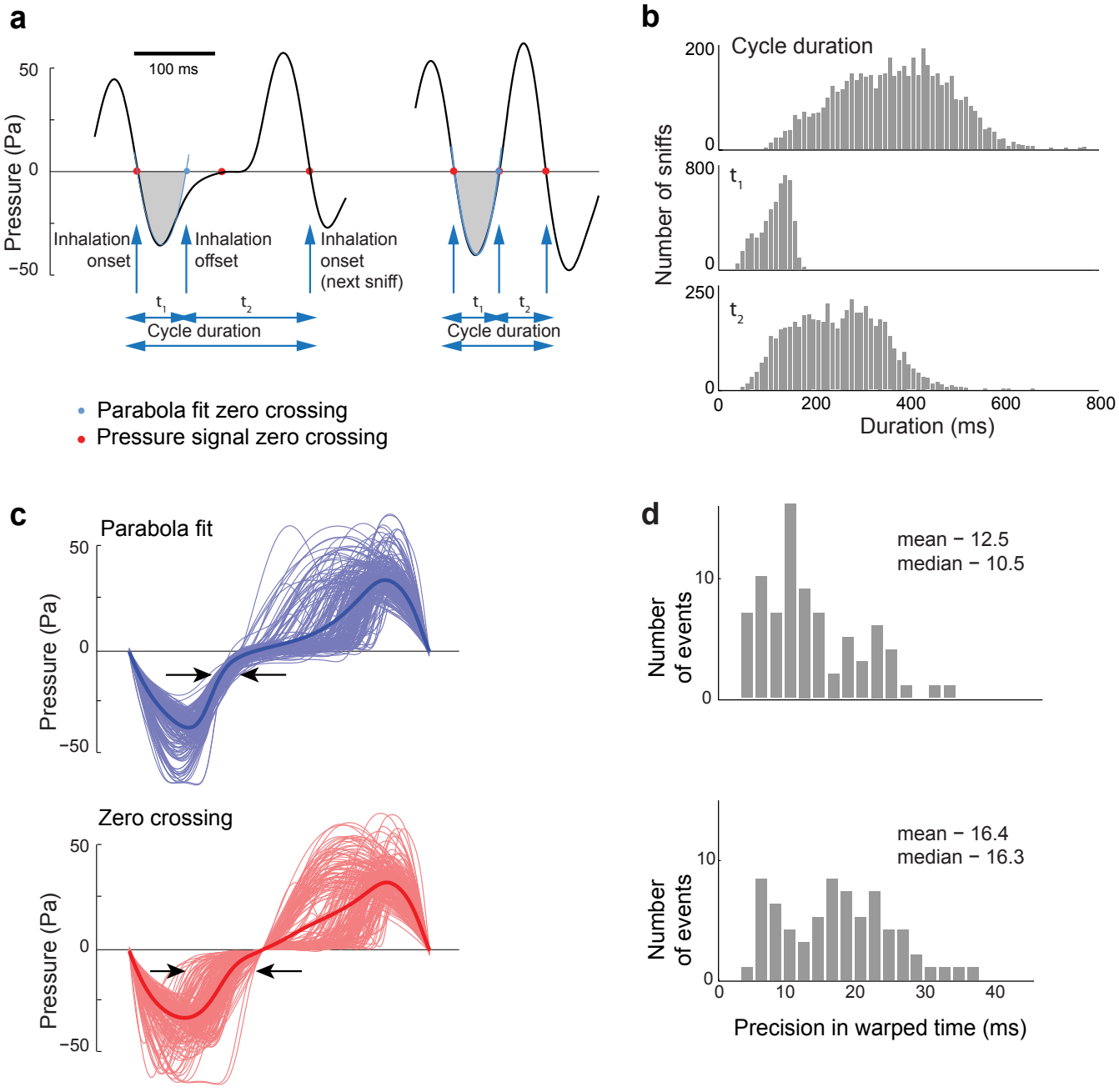

Supplementary Figure 2. Sniff warping analysis. **a.** Pressure waveforms of two typical sniffs: normal and fast. Blue line is parabolic fit to the first minimum after the inhalation onset. Red dots indicate pressure signal zero crossing, blue dots are parabola fit zero crossing. Gray area is an inhalation interval defined by the parabola fit zero crossing. **b.** The distributions of the full sniff cycle durations, the durations of inhalation intervals, τ_1, and the duration of the second part of the sniff, τ_2 (sniffs from one animal in one session). The offset of the inhalation was defined by the second parabola fit zero crossing (blue dots). **c.** Sniff warping for two methods of defining the onset of inhalation: by the parabola fit zero crossing (blue) and by pressure signal zero crossing (red). The thick lines are average warped sniff waveforms, thin lines are examples of individual waveforms. **d.** The distribution of the precision for corresponding warping procedures.

Nature Neuroscience doi:10.1038/nn.2877

All sniffs can be roughly divided into two groups, normal and fast (Supplementary Fig. 2a). The normal sniff consists of inhalation interval, pause, and exhalation interval. Fast sniffs usually lack the pause interval. (Note, that the sequence of the sniff phase in our case in awake mouse is different from that observed in anesthetized mouse. In the later state, mouse inhaling, exhaling and then pause.) The beginning of the inhalation interval and the end of the exhalation interval can be defined by falling zero crossing of the pressure signal. At this time point the relative pressure in the nasal cavity changes sign, which means that airflow changes direction from exhalation to inhalation. The end of the inhalation interval and the beginning of the exhalation period are less obvious, because the pressure signal flattens during the pause interval and the accuracy of zero crossing time point is low.

We tried a few methods of sniff-to-sniff alignment:
1) We uniformly stretched or compressed the whole sniff cycle.
2) We divided the sniff cycle into two intervals: the inhalation phase and the rest of the sniffing cycle. The end of the inhalation phase has been defined by parabola fit zero crossing. We independently stretched or compressed each interval (Fig. 1b and Supplementary Fig. 2a).
3) Similarly to method #2, but the end of inhalation cycle was defined by rising zero crossing of the pressure signal (Supplementary Fig. 2a).
4) We divided the sniff cycle into three intervals: the inhalation phase, pause, and exhalation phase. The inhalation phase was defined as in method #2. The onset of the exhalation phase was defined by zero crossing of parabola fit of the exhalation peak (not shown). And the pause was an interval between inhalation and exhalation. For fast sniffs the pause interval has zero length.

We do not think that any of these transformations are optimal. The optimal transformation would yield the time course of odors reaching receptors. This transformation is unknown and requires further study. For all analysis in the paper we employ the two-interval procedure (method #2). Our motivation was the following: Individual sniffs vary a lot, and we can roughly separate them into two groups: normal and fast sniffing (Supplementary Fig. 2a,b). The common feature of all sniff waveforms is the presence of the first inhalation phase. Inhalation can be followed either directly by exhalation, or by a pause, where the slope of the pressure signal flattens, which is then followed by exhalation. The temporal warping by stretching or compressing the whole length of the sniffing interval (method #1) fails to reveal the interesting structure, mainly due to the fact that scaling of the inhalation phase and the rest of the sniffing cycle can be quite different. Increasing the number of warp points to give a three-interval warping procedure (method #4) does not reveal much more structure in the neuronal responses, as the majority of sharp events and initial excitatory or inhibitory events happened during the first phase.

We specifically compared warping methods #2 and #3. Both methods are based on two interval warping. The averaged warped sniff waveforms and individual examples are presented on Supplementary Fig. 2c. For both methods, we estimated the distributions of temporal precision of sharp responses (Supplementary Fig. 2d). Both temporal precision distributions were significantly shifted to smaller values compared to the distribution obtained with no warping ($p = 7.3e-7$ and $p = 4.6e-8$ for pressure signal zero crossing and parabola fit zero crossing methods, Kolmogorov-Smirnov test). However, the parabola crossing method demonstrates higher temporal precision than the pressure signal zero crossing method (Supplementary Fig. 2d, Kolmogorov-Smirnov test, $p=9.1e-4$). This result can be explained by two reasons. First, the exact position of the pressure signal zero crossing is poorly defined due to the very shallow slope of the pressure signal at the majority of the sniffing cycles. Second, the width of the

actual waveform spread during is larger for the second method, especially the end of the inhalation phase. These widths are indicated in Supplementary Fig. 2c with black arrows.

We do not claim that the method we used (#2) is the best possible method, however, it reveals the essence of the warping phenomena. Finding the optimal transformation to recover phase from the pressure signal is beyond the scope of the current work, but provides an interesting problem for future work.

Supplementary Table 1. Statistical parameters of sniffing signal for different sessions.

sess #	Inhalation interval duration (ms)		Whole sniff cycle duration (ms)	
	mean	std	mean	std
1	118	32	369	116
2	111	36	358	126
3	116	29	373	116
4	111	30	364	114
5	80	17	247	61
6	161	97	293	131
7	125	46	466	146
8	108	43	462	191
9	103	25	323	72
10	96	18	300	58
11	119	39	381	122
all sessions:	**111**	**44**	**358**	**131**

Nature Neuroscience doi:10.1038/nn.2877

III. Diversity of spontaneous activity patterns

We analyzed spontaneous firing rates of 66 cells, using a temporal warping procedure. To estimate average spontaneous activity we used a five sniff time interval preceding the odor delivery for all trials. Three examples of firing rate dependences for these unodorized sniffs are shown on Supplementary Fig. 3a–c. The overall distribution of average background firing rates is shown in Supplementary Fig. 3d. The mean and standard deviation of background firing rates are 16.2 Hz and 8.0Hz. To characterize the level of modulation of firing rate by the sniffing cycle we fit the data with the zero and the first Fourier terms: $a_0 + \mathrm{Re}\left[a_1 \exp\left(2\pi i t / T_{sniff}\right)\right]$ (Supplementary Fig. 3a–c). The level of modulation is a ratio between the absolute value of the first Fourier component, $|a_1|$, and average firing rate a_0. The value $|a_1|/a_0 = 0$ corresponds to the absence of modulation, see example at panel C, $|a_1|/a_0 = 0.04$. Examples in panels **a** and **b** have modulation of 0.79 and 0.34, respectively. Distributions of average firing rates and modulation coefficients reveal no obvious separation of cell groups based on these parameters.

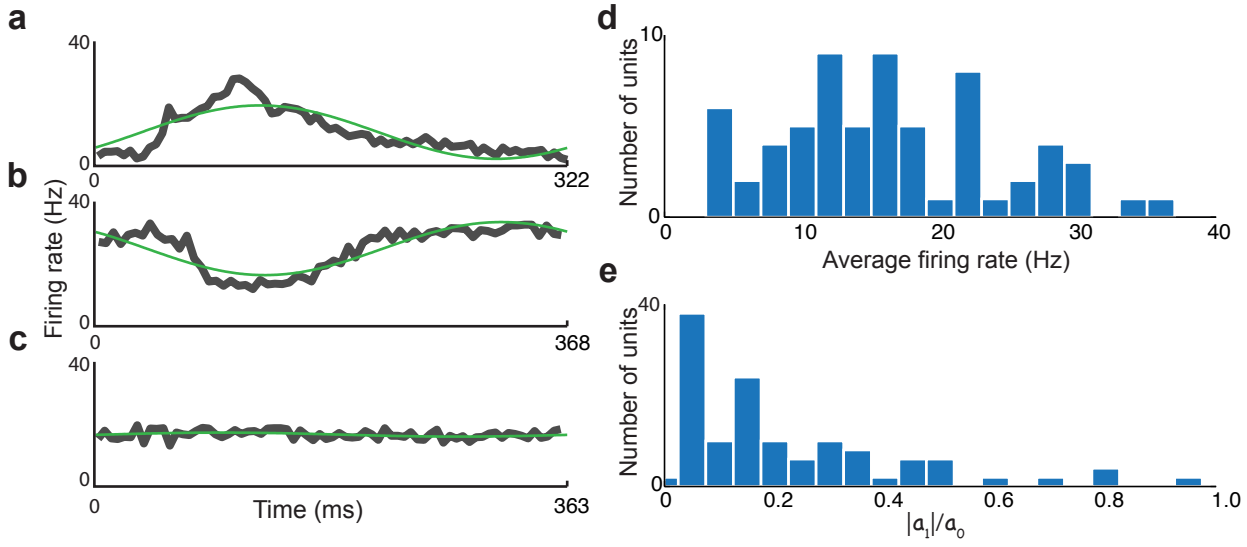

Supplementary Figure 3. Modulation of spontaneous firing rate. **a-c.** Three examples of spontaneous firing rate modulation relative to the sniffing cycle (thick gray lines). The data fits by the zero and the first Fourier components are shown by green lines. **d**. Distribution of average firing rates. **e**. Distribution of ratios between the amplitudes of the first and zero Fourier components, as a measure of level of firing rate modulation.

Supplementary Table 2. Excitatory and inhibitory responses. The table shows the distribution of the excitatory (green), inhibitory (blue) and no (black) responses for 7 mice, 11 sessions and 66 units. The absence of a dot means that this cell was not presented with this odor. The black circles around colored dots indicate responses for which the number of spikes in one sniff is statistically the same with and without stimulus presentation (see Methods). These responses most probably would not be seen without sniff alignment. The list of odors used in all sessions is presented on the left column.

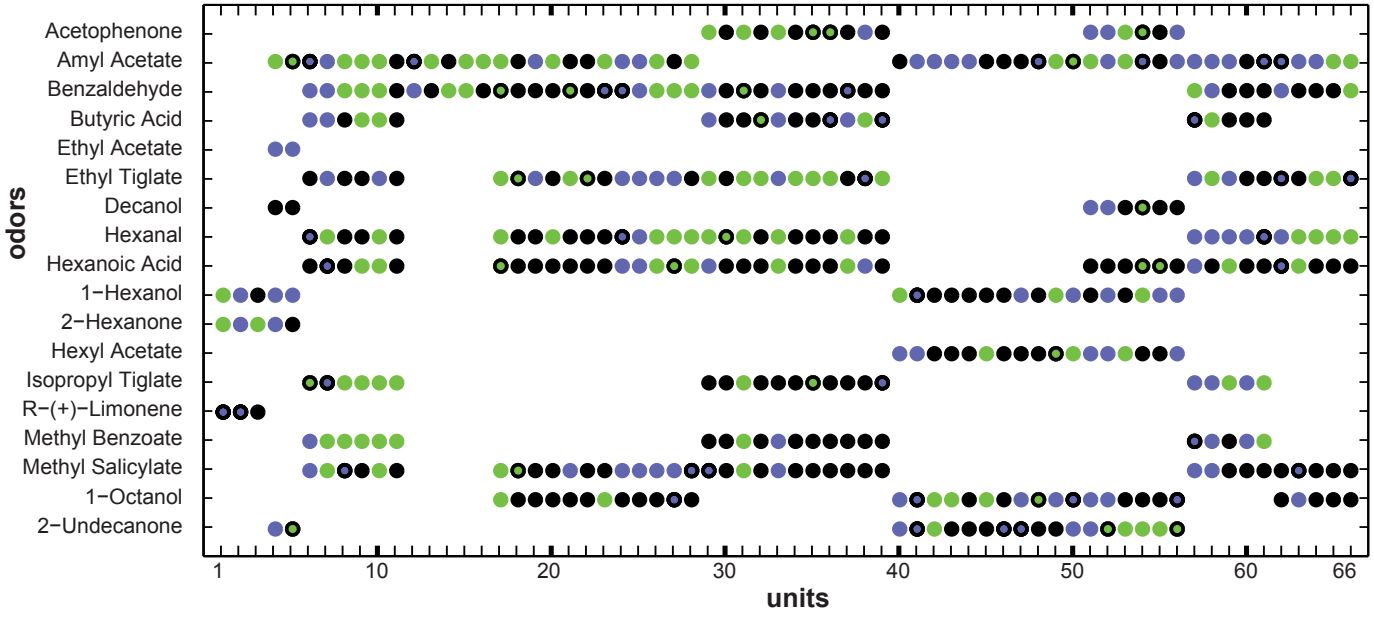

Nature Neuroscience doi:10.1038/nn.2877